J Shoulder Elbow Surg (2020) 29, e478–e490

ELSEVIER

Journal of Shoulder and Elbow Surgery

www.elsevier.com/locate/ymse

In vivo testing of an injectable matrix gel for the treatment of shoulder cuff muscle fatty degeneration

Tai Huynh, BS[a], John Taehwan Kim, PhD[a], Grady Dunlap, BS[a], Shahryar Ahmadi, MD[b], Jeffrey C. Wolchok, PhD[a,b,*]

[a]*Department of Biomedical Engineering, University of Arkansas, Fayetteville, AR, USA*
[b]*College of Medicine, Orthopedic Surgery, University of Arkansas for Medical Science, Little Rock, AR, USA*

Introduction: Extracellular matrix (ECM) gels have shown efficacy for the treatment of damaged tissues, most notably cardiac muscle. We hypothesized that the ECM gel prepared from skeletal muscle could be used as a treatment strategy for fatty shoulder cuff muscle degeneration.
Methods: We conducted experiments to (1) evaluate host biocompatibility to ECM gel injection using a rat model and (2) examine the effect of ECM gel injection on muscle recovery after delayed repair of a released supraspinatus (SSP) tendon using a rabbit model.
Results: The host biocompatibility to the ECM gel was characterized by a transient rise (first 2 weeks only) in several genes associated with macrophage infiltration, matrix deposition, and inflammatory cytokine production. By 8 weeks all genes had returned to baseline levels and no evidence of fibrosis or chronic inflammation was observed from histology. When gel injection was combined with SSP tendon repair, we observed a significant reduction (7%) in SSP muscle atrophy (24 + 3% reduction from uninjured) when compared with treatment with tendon repair only (31 + 7% reduction). Although fatty degeneration was elevated in both treatment groups, fat content trended lower (2%) in response to combined tendon repair and intramuscular ECM injection (4.1 + 2.1%) when compared with tendon repair only (6.1 + 2.9%). Transcriptome analysis revealed adipogenesis and osteoarthritis pathway activation in the repair only group. These key pathways were abrogated in response to treatment using combined repair plus gel.
Discussion: The findings suggest that ECM injection had a modest but positive effect on muscle mass, fatty degeneration, and key cellular signaling pathways.
Level of evidence: Basic Science Study; Biomechanics; Histology; Microbiology In Vivo Animal Model

Keywords: Rotator cuff tear; fatty infiltration; fatty degeneration; extracellular matrix; injectable ECM; rabbit supraspinatus; RNA-seq; biomaterial

In selected cases, the surgical care for damaged rotator cuffs is reattachment of the torn tendon(s) to their original boney insertion sites on the humerus.[5,34,49] Despite significant progress with arthroscopic techniques and improved fixation devices, rotator cuff surgery failure rates remain high, reported to be around 30%-35%.[23,28,31] The muscles of the rotator cuff undergo progressive fatty degeneration, also termed fatty infiltration, after tendon tear.[15,17] This pathologic degeneration of shoulder muscle in patients with rotator cuff tears is shown to be a contributing factor to the

All animal procedures were approved by the Institutional Animal Care and Use Committee of the University of Arkansas (#19002 and #3655).

*Reprint requests: Jeffrey C. Wolchok, PhD, Department of Biomedical Engineering, University of Arkansas, 700 W. Research Blvd., Fayetteville, AR 72701, USA.).

E-mail address: jwolchok@uark.edu (J.C. Wolchok).

1058-2746/$ - see front matter
https://doi.org/10.1016/j.jse.2020.03.038

high failure rate.[19] Although surgical techniques have been developed to address the torn tendinous portion of the damaged rotator cuff, there are currently no effective methods to address fatty degeneration. Fatty degeneration remains a well-recognized but currently unaddressed pathologic condition that limits the success of rotator cuff surgery.[10,14,41,57] Our goal is the development of an effective treatment for the repair of fatty degenerated rotator cuff muscle that could become an adjunct to the current tendon repair techniques.

Under the right conditions, skeletal muscle has a robust capacity for self-repair. After mild muscle injury (eg, strains, contusions, and lacerations) cells may be injured, but the damaged underlying extracellular matrix (ECM) persists at the site of injury and regeneration is robust and complete.[24,39] Growth factors released from injured muscle matrix promote satellite cells residing between myofibers to migrate to sites of injury, re-enter cell cycle, proliferate, and differentiate into myoblasts, which, in turn, undergo fusion to form nascent myofibers.[2,52] However, when muscle tissue is lost, the structural cues produced by the ECM are missing and regeneration is instead marked by fibrosis and the formation of noncontractile scar tissue.[3,29,53] The differential response to mild and severe muscle injury suggests an important role for ECM as a trigger for muscle regeneration. To deliver ECM cues into fatty infiltrated muscle, we are proposing the utilization of an injectable, water-based, matrix gel prepared from skeletal muscle tissue. Our enthusiasm for a matrix gel approach as a muscle repair strategy was motivated not only by the recognized role of matrix during muscle healing, but also by the cardiac work of Dr. Christman's group at the University of California at San Diego. They have developed an injectable matrix gel using cardiac tissue and demonstrated that injection of the material into infarcted cardiac muscle tissue stimulated regeneration.[49-51] A possible mechanism of repair is ECM gel promotion of vessel formation/perfusion, endothelial cell/muscle progenitor cell infiltration, and muscle cell proliferation.[9,43] We believe that the same regenerative results that have been reported in infarcted cardiac muscle tissue could be translated to fatty degenerated skeletal muscle.

We conducted this study to deeply explore the safety and efficacy of an injectable ECM gel while also deciphering whether any key wound healing mechanisms were impacted by matrix gel implantation. Specifically, we designed the study to test the hypothesis that intramuscular delivery of the matrix gel triggers the activation of pro-myogenic wound healing pathways that ameliorate fatty muscle infiltration. To test this hypothesis, we conducted experiments to (1) examine the longitudinal host response (biocompatibility) to ECM gel injection into normal muscle using a rodent model and (2) test matrix gel regenerative performance in a well-accepted[20,21,45,46] animal model of delayed rotator cuff repair (rabbit).

Methods

ECM gel preparation

Human quadriceps muscle (Science Care, Phoenix, AZ, USA) was thawed, trimmed to remove fat and connective tissue, and decellularized in 1% (wt/vol) solution of sodium dodecyl sulfate in phosphate buffered saline (PBS) with agitation and multiple solution exchanges for up to 2 weeks[9,27] (Fig. 1, *a* and *b*). We then rinsed the tissue with deionized water and incubated in a DNase/RNase solution overnight at 4°C with agitation. The remaining ECM was rinsed, lyophilized, flash-frozen using liquid nitrogen, and ground into a fine powder. We digested the ECM powder using a pepsin solution (1 mg/mL pepsin in 0.1 M HCl) at a ratio of 10 mg ECM/1 mL pepsin at a pH of 2.4 (adjusted every 12 hours if necessary) for 48 hours at room temperature[9,56] (Fig. 1, *c* and *d*). The solubilized ECM solution was neutralized (pH = 7.4) and diluted to a concentration of 10 mg/mL in PBS. Finally, we loaded the neutralized pregel solution into syringes and stored it at −20°C (Fig. 1, *e* and *f*).

Host response

Adult (12-14 weeks old) Sprague Dawley rats (Harlan, Indianapolis, IN, USA) (n = 12), weighing approximately 325-350 g, were used as the animal model to explore the host response to injected ECM. We used isoflurane for anesthesia with induction dosage of 4% and maintenance dosage of 2% in oxygen. Syringes containing ECM gel were thawed and injected (200 μL; 27-gauge needle) into the tibialis anterior (TA) at 5 sites along its distal-to-proximal length intramuscularly through the skin. We injected the contralateral TAs with sterile PBS to serve as comparative controls. Postoperative analgesia consisted of 0.1 mg/kg buprenorphine administered subcutaneously via injection twice daily for 2 days. A single surgeon performed all procedures. Animals also had access to anti-inflammatory medication (Rimadyl; 2 mg/d) via a dietary tablet (Rodent MD's, Bio Serv, Flemington, NJ, USA). We added tablets daily to each cage for 1 week after surgery in accordance with Institutional Animal Care and Use Committee (IACUC)-approved protocols and housed animals individually in standard-sized cages with unrestricted movement. The animals were allowed to bear weight on the operative extremity as tolerated. All animals were housed for a 3-, 14-, or 56-day recovery period (n = 4 animals/time point).

Rotator cuff repair

Adult (24 weeks old) male New Zealand white rabbits (pre-surgery mass approximately 3.5 kg) purchased commercially (Charles River) (n = 14) were used to examine the effect of ECM gel injection on recovery from torn rotator cuff repair. The rotator cuff tear and delayed tendon repair surgeries were performed following published methods.[37,42] A trained orthopedic surgeon performed the surgeries. We used isoflurane for anesthesia with the induction dosage of 5% and the maintenance dosage of 3% in oxygen. The left shoulder was shaved and disinfected. A longitudinal incision was made over the shoulder, and dissection performed down to the deltoid. The deltoid was retracted to reveal the supraspinatus (SSP) tendon. The SSP tendon was transected at its insertion onto the greater tuberosity. The cut end of the tendon was

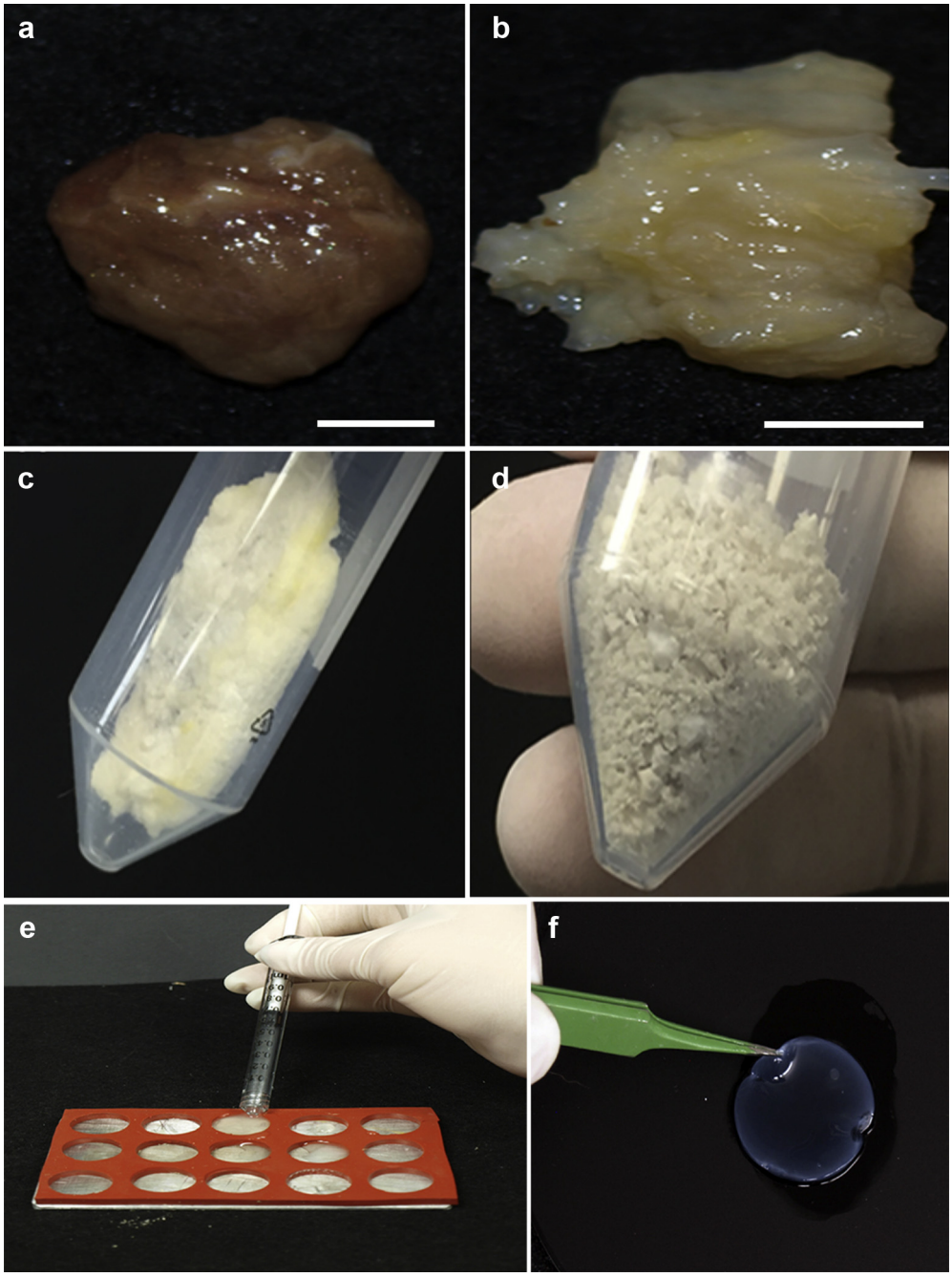

Figure 1 (**a**) Human quadriceps muscle was (**b**) decellularized, (**c**) lyophilized, (**d**) ground into a fine powder, and (**e**) pepsin digested to create an injectable pregelled matrix solution. (**f**) The pregelled muscle matrix solution forms a gel when warmed to 37°C.

tagged with a nonresorbable No. 4-0 suture (Prolene; Ethicon, Somerville, NJ, USA) for later identification. All attachments of the tendon to the surrounding tissues, including the infraspinatus, were released, allowing the tendon to retract freely away from its insertion site. The incisions were closed with interrupted, subcutaneous No. 3-0 Vicryl sutures (Ethicon), and the skin was closed with a running 4-0 monocryl suture (Ethicon). The contralateral shoulder remained untreated to serve as a comparative control. All animals were housed for a 12-week recovery period.

After recovery, all animals underwent SSP tendon reattachment repair surgery. The free tendon edge was identified by use of the tag suture and double stitched to the humerus using a fiber wire suture. We randomly assigned half of the animals to receive 1 mL of muscle-derived ECM gel injection into the SSP muscle at 5 locations along its length. After repair, the surgeon closed the surgical site with a suture as previously described. The animals were maintained in the animal facility for a recovery period of 12 weeks (n = 7/treatment group). At the end of the recovery period, a veterinarian euthanized all animals via intracardiac injection of a commercial euthanasia solution. SSP muscles were harvested, weighed, imaged, and prepared for histologic sectioning and gene expression testing.

Contractile force measurements (rat only)

At each postinjection time point (3, 14, and 56 days), we measured peak tetanic TA contractile torque in situ using published methods familiar to our group.[29] The ankle was flexed to 90°, and the foot was secured to the lever arm of a commercial muscle physiology system (Aurora Scientific, Ontario, Canada). We measured the TA peak isometric tetanic torque by stimulating the peroneal nerve with the aid of a physiological stimulator (Grass; S88) and determined optimal voltage (2-5 V) using a series of tetanic contractions (150 Hz, 0.1 ms pulse width, 400 ms train). We recorded raw peak tetanic contractile force (N) from both the treated and contralateral control limb of each animal. We calculated peak tetanic force for each animal using the average of 4 contractions and reported the animal weight normalized force data (N/kg body weight) in the results. At the conclusion of electrophysiological testing, we harvested the TA muscles and euthanized the rats by carbon dioxide inhalation.

Histologic analysis

Muscle tissue (rat and rabbit) was flash frozen in isopentane (2-methylbutane) chilled in liquid nitrogen. Tissue was sectioned (8 μm) with the aid of a cryostat (Leica BioSystems) and mounted onto microscopic slides. Slides were immunostained using primary antibodies (1:300; Novus Biologicals) directed against collagen III (IgG), or collagen I (IgG) with or without myosin heavy chain costain, followed by incubation in the appropriate fluorescently labeled secondary antibodies (AlexaFluor, 1:300; Life Technologies). Additional tissue sections were stained using hematoxylin and eosin (H&E) or oil red-O following the manufacturer's guidelines (Sigma-Aldrich). All sections were digitally imaged (100×, Nikon CiL).

Tissue immunoreactivity to collagen I as a percentage of total tissue area (% collagen I) was calculated with the aid of image analysis software (ImageJ) using techniques familiar to our group.[29] Similar image analysis methods were used to compute the fiber cross-sectional area (μm^2) using the collagen III positive area. Oil red-O images were evaluated using an in-house developed MATLAB code to isolate oil red-O positive (fat) and negative (muscle) tissue regions within each section. The ratio of the oil red-O positive tissue area to the total tissue area was used to calculate the intramuscular fat area fraction (% area).

Gene expression

RNA was extracted from tissue samples using the RNeasy Kit (Invitrogen). Commercially available TaqMan primers (Invitrogen) for Pax7, MyoD, MyoG, Col I, Col III, TGF-β1, IL-6, IL-10, CD68, and 18s ribosomal housekeeping were used to quantify the expression of desired host-response genes from rat tissue. Expression was normalized to 18S and then referenced to the contralateral saline injected limb. Commercially available SYBR Green primers (Bio-Rad) for PPAR-γ, MURF1 (Trim63), Pax7, MyoG, and RPL4 housekeeping were used to quantify the expression rabbit muscle genes. Experimental sample group (n = 6-7/group) expressions were normalized to RPL4 and then referenced to the contralateral uninjured limb. Gene expression levels are reported as fold change using the $2^{-(\Delta\Delta Ct)}$ method.

The full transcriptomes of representative repair only, repair plus ECM gel, and uninjured controls rabbit SSP muscle samples (n = 5/group) were analyzed using RNA-Seq. cDNA libraries were sequenced on the NextSeq500 platform (Illumina) to a mean depth of 20 million reads per library. RNA sequencing reads were mapped to the *Oryctolagus cuniculus* genome (OryCun2.0) from NCBI using the 2-pass STAR protocol.[11] Reads were quantified using FeatureCounts,[34] followed by the analysis of differential expression and normalization in edgeR.[44] Differential expression was selected using a maximum false discovery rate of 0.25 and a minimum log fold change of 1.5. Pathway level analysis was also performed using Ingenuity Pathway Analysis (IPA) (Qiagen).[32]

Statistical analysis

All data are presented as the mean and standard deviation unless otherwise noted. The effect of treatment on TA mass, TA contractile force, TA collagen I area (%), TA myofiber cross-sectional area, TA and SSP gene expression, and SSP mass reduction was evaluated using a 2-sided Student's *t*-test. The effect of treatment SSP fat area fraction, SSP collagen I area fraction, and SSP myofiber area was evaluated using analysis of variance with Tukey's post hoc test. A standard $P < .05$ level of significance was used as the threshold for all statistical tests.

Results

Host response

All animals tolerated the ECM gel injection treatment well. Peak tetanic contractile force values for ECM gel–injected TA muscle were statistically indistinguishable from PBS controls at 3 days (0.97 + 0.41 vs. 0.72 + 0.18 N/kg) and at 14 days (1.72 + 0.87 vs.1.34 + 0.56 N/kg) postinjection (Fig. 2, *a*). However, at 56 days, the study endpoint, a statistically significant ($P = .048$) increase in contractile force was detected for the ECM gel injection group. Mean gel-injected TA contractile force values were on average 53 + 37% higher than PBS-injected control values (3.25 + 0.41 vs. 2.25 + 0.70 N/kg). TA mass followed a similar trend to force. At 3 days (1.93 + 0.23 vs. 2.14 + 0.16 g/kg) and 14 days (2.03 + 0.08 vs. 2.09 + 0.09 g/kg) postinjection, TA mass did not differ between the ECM gel- and PBS-injected groups, respectively (Fig. 2, *b* and *c*). Similar to force results, at 56 days, there was a statistically significant ($P = .003$) increase (18 + 8%) in TA mass for the ECM gel injection group (2.43 + 0.14 g/kg) when compared with PBS controls (2.05 + 0.07 g/kg).

Rat TA sections immunostained for collagen I exhibited no discernible differences between ECM gel injection and PBS controls across all time points (Fig. 3, *a*). There were no indications of abnormal inflammatory or fibrotic responses within any of the TA tissue sections examined. Fiber cross-sectional area as indicated by collagen III–positive regions was normal in appearance with spheroid muscle fiber cross-sections observed for both

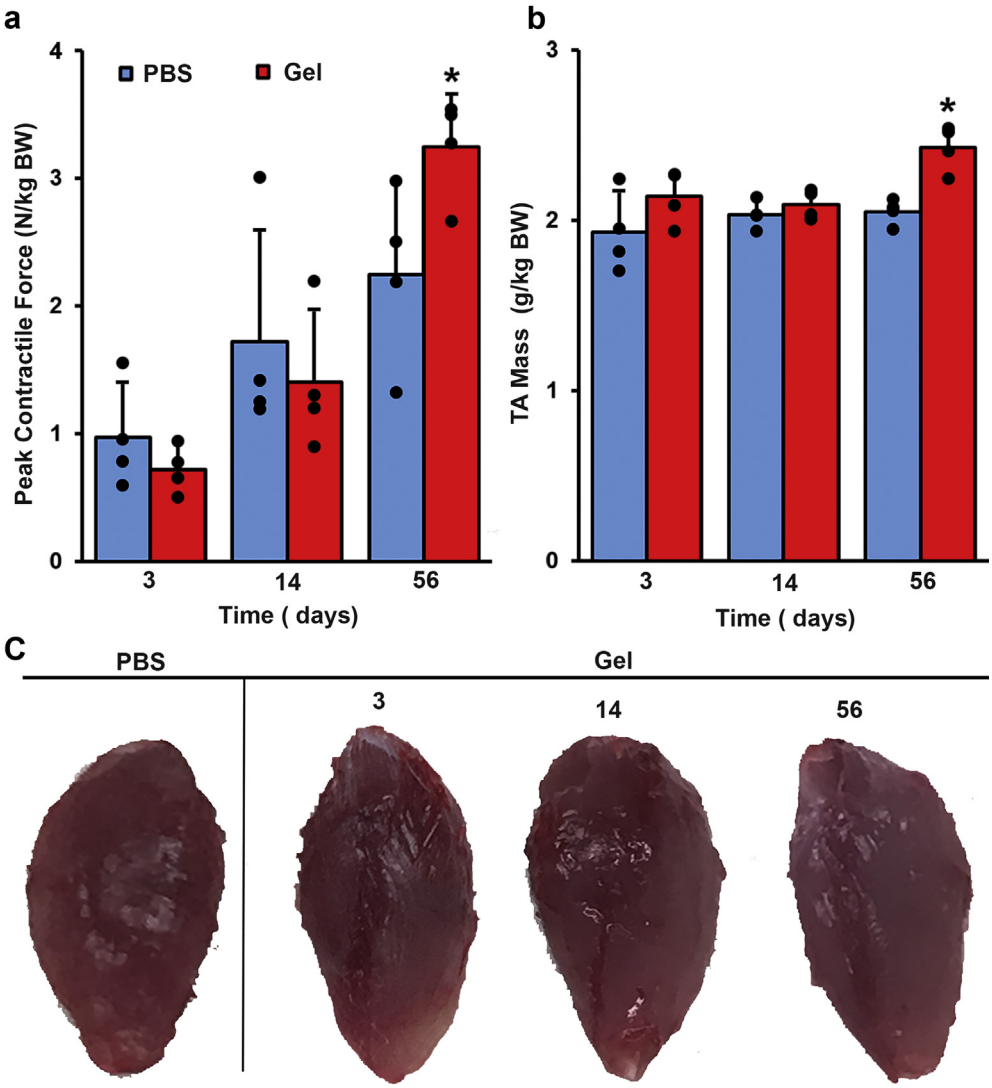

Figure 2 (**a**) TA muscle peak contractile force (N/kg body weight) and (**b**) wet weight (g/kg body weight) data normalized to animal weight. (**c**) Gross morphology of TA muscles 56 days after PBS injection (left) and 3, 14, and 56 days after ECM gel injection (right). Data are presented as group means + SD; n = 4/group; *denotes statistically significant ($P < .05$) differences from controls. *TA*, tibialis anterior; *PBS*, phosphate buffered saline; *ECM*, extracellular matrix; *SD*, standard deviation.

groups (Fig. 3, *b*). H&E staining also appeared normal with tightly apposed bundles of myofibers and no evidence of hyperplastic regions within any of the TA sections (Fig. 3, *c*). Collagen I–positive area fraction (Fig. 3, *d*) and myofiber cross-sectional area (Fig. 3, *e*) were not significantly different between either groups at any time point.

The expression levels of genes associated with ECM and ECM regulation, Col I (0.031), Col III ($P = .017$), and TGF-β1 ($P = .012$), were all significantly upregulated (approximately 10-fold) at 3 days postinjection (Fig. 4, *a*). By 14 days postinjection, Col III ($P = .035$) and TGF-β1 ($P = .017$) remained upregulated by approximately 5-fold in the gel-injected groups compared with controls until returning to basal levels of expression by 56 days. We observed a similar trend in a panel of inflammatory genes, with IL-6 ($P = .033$) and IL-10 ($P = .025$) being expressed approximately 15-fold higher in response to gel injection at 3 days postinjection when compared with PBS controls, whereas CD68 ($P = .049$), a macrophage-specific marker, was expressed approximately 50-fold higher in the gel group compared with PBS controls at the same time point (Fig. 4, *b*). By 14 days, all gene expression related to these targets returned to PBS control tissue levels. Myogenic gene expression (Pax7, MyoD, MyoG) is statistically indistinguishable between the 2 treatment groups at all postinjection time points (Fig. 4, *c*).

Rotator cuff repair

All animals tolerated the rotator cuff (RC) surgery, bore weight normally on the treated limb by the end of the first postoperative week, and gained weight throughout the

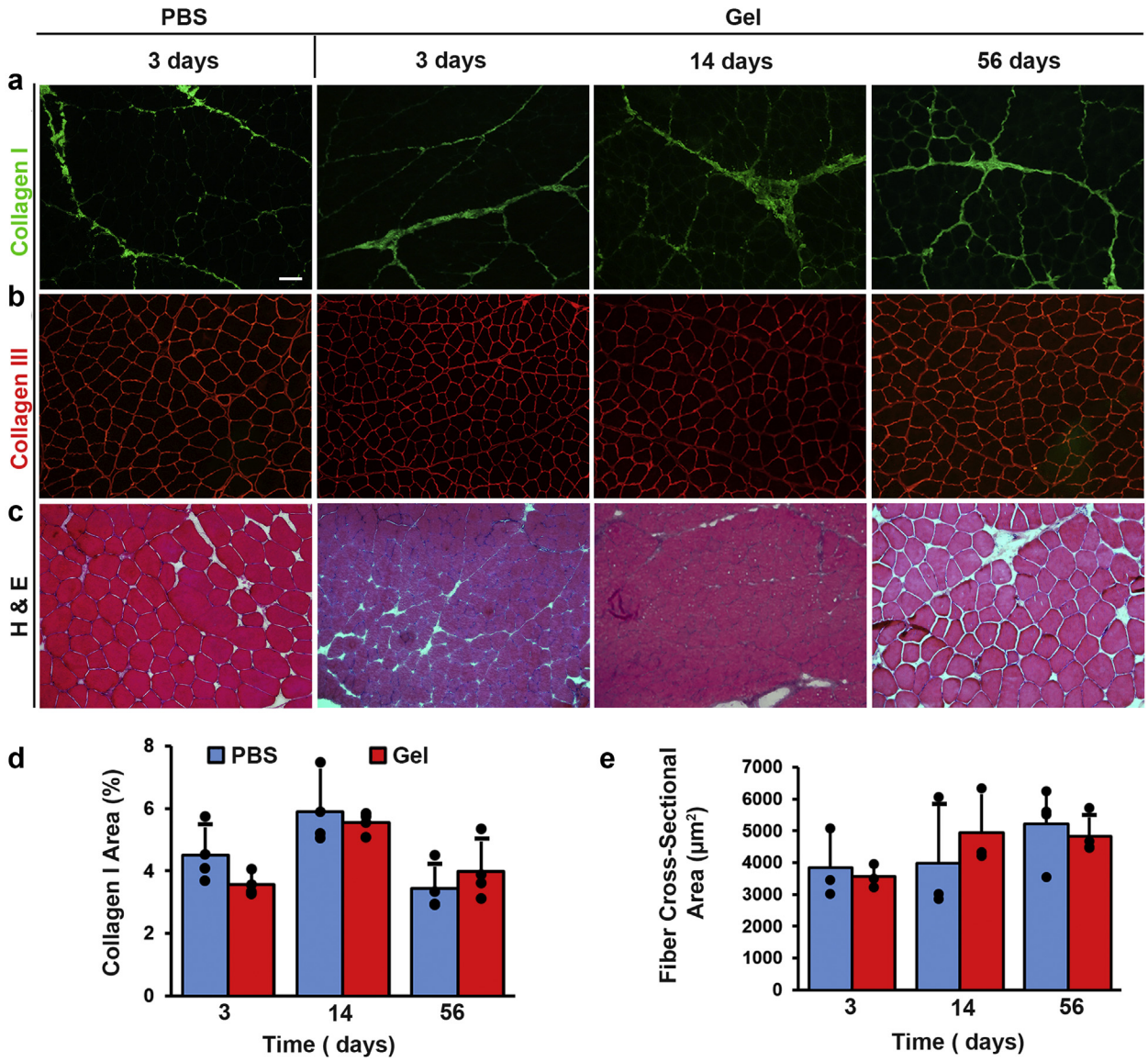

Figure 3 TA muscle cross-sections were stained for (**a**) collagen I (green), (**b**) collagen III (red), and with (**c**) hematoxylin and eosin (H&E). Representative 56 days after PBS injection (left) and 3, 14, and 56 days after ECM gel injection TA cross-sections are presented. Scale bar = 100 μm unless noted. Cross-sections were quantified for (**d**) collagen I area fraction and (**e**) muscle fiber cross-sectional area. Group means + SD are presented; n = 4/group. *TA*, tibialis anterior; *PBS*, phosphate buffered saline; *ECM*, extracellular matrix; *SD*, standard deviation.

study period. Animal growth rate was examined during the 12 weeks before and after SSP treatment. Although growth generally slowed with increasing animal age, we did not detect any differences in growth rate between repair only and repair plus ECM gel groups during either the 12 weeks before repair or during the 12 weeks after repair. At the study endpoint (12 weeks after repair), a layer extramuscular fat remained on muscles harvested from both tendon repair only and combined tendon repair plus ECM gel treatment animals (Fig. 5, *a*). No accumulation of extramuscular fat was observed on any of the uninjured contralateral SSP muscles. Although both treatment strategies resulted in significant muscle atrophy when compared with uninjured contralateral controls, combined tendon repair with ECM gel injection treatment had a positive effect on SSP mass to decrease atrophy. Treatment with tendon repair only resulted in a 31 + 7% reduction in SSP mass when compared with uninjured controls. Alternatively, treatment using combined tendon repair plus ECM gel injection resulted in a 24 + 3% reduction in SSP mass, a decrease of 7% when compared with the repair only (Fig. 5, *b*). The SSP mass reduction between the repair only and the combined repair plus ECM injection groups was statistically significant.

Oil red-O staining of uninjured, repair only, and repair with ECM gel injection SSP sections revealed elevated levels of

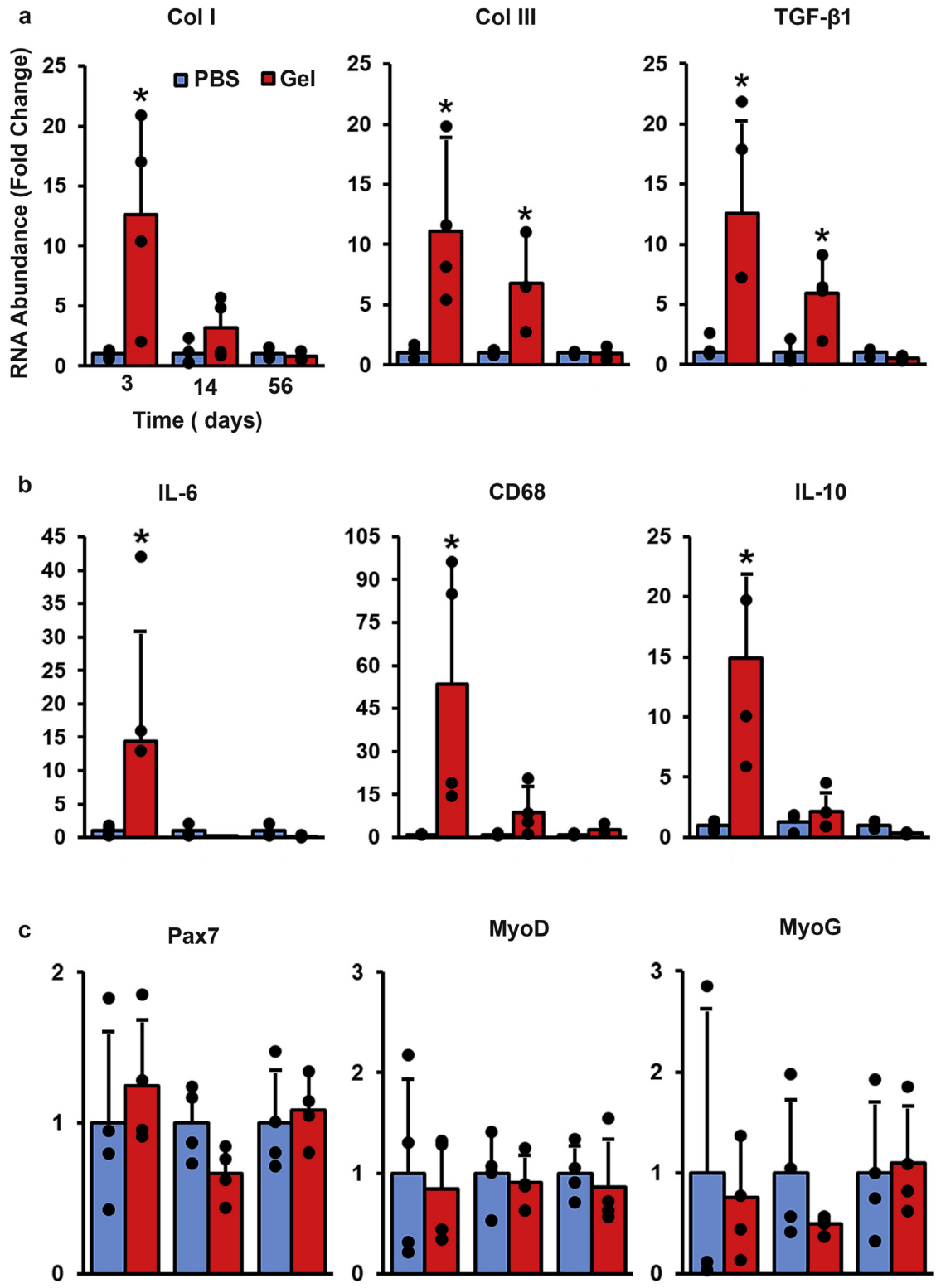

Figure 4 Comparison of relative gene expression for PBS- and ECM gel–injected groups determined using qRT-PCR. The expression of (**a**) ECM (Col I and Col III), ECM regulatory (TGFβ1), (**b**) inflammation (IL-6), anti-inflammation (IL-10), macrophage marker (CD68), and (**c**) myogenic (Pax7, MyoD, MyoG) genes were measured using muscle tissue harvested from the TA of each animal tested. Expression is presented as fold change normalized to PBS-injected muscle expression. Group means + SD are presented, n = 3-4/group. *denotes statistically significant ($P < .05$) differences from controls. *PBS*, phosphate buffered saline; *ECM*, extracellular matrix; *qRT-PCR*, quantitative real time polymerase change reaction; *TA*, tibialis anterior; *SD*, standard deviation.

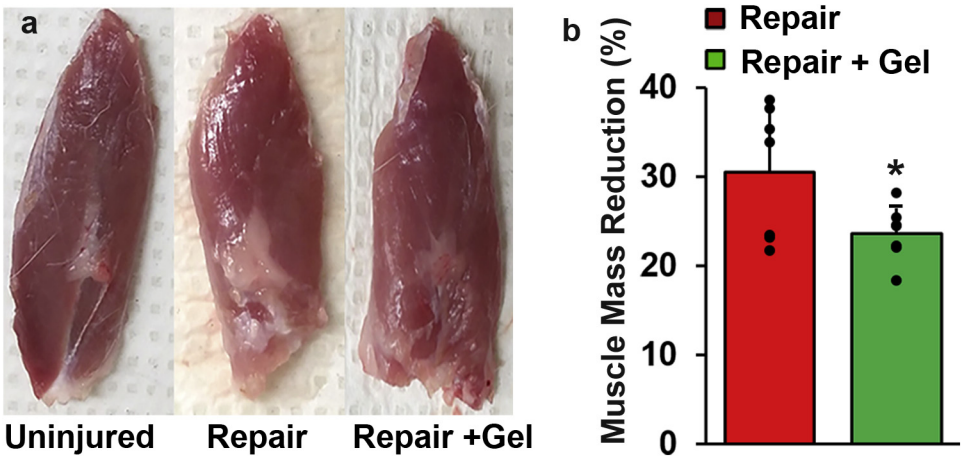

Figure 5 (**a**) Gross morphology of representative SSP muscles from the uninjured, repair only, and combined repair plus ECM gel groups is presented to show the appearance of surface fat accumulation on injured muscles. (**b**) SSP muscle wet weight data (% of uninjured) for the repair only and combined repair plus ECM gel groups. Data are presented as group means + SD; n = 7/group; *denotes statistically significant ($P < .05$) differences between groups. *SSP*, supraspinatus; *ECM*, extracellular matrix; *SD*, standard deviation.

intramuscular lipids within muscle tissue collected from both treatment groups (Fig. 6, *a*). The repair only and combined repair with ECM gel sections contained a gradient of intramuscular fat with the densest regions localized nearest the tendon injury site. Qualitative examination of sections immunostained for collagen I or collagen III revealed no notable differences between either of the treatment groups or differences from uninjured controls (Fig. 6, *b* and *c*). Collagen I and III immunoreactivity was uniformly distributed around muscle fibers (collagen III primarily) and multifiber bundles (collagen I) for all treated and uninjured control muscles examined. We did not detect any abnormal changes to myofiber cross-sectional morphologies between the treatment groups. H&E sections from both treatment groups consistently exhibited a lack of tight myofiber apposition when compared with sections prepared from contralateral normal tissue and further confirmed fiber atrophy due the rotator cuff tear (Fig. 6, *d*).

Quantitative image analysis of oil red-O-stained sections revealed that both repair and repair with ECM gel treatments resulted in significant increases in intramuscular fat area fraction when compared with uninjured contralateral controls. Fat fraction of repair only group was 6.1 + 2.9%, whereas repair plus ECM gel fat fraction was 4.1 + 2.1%, a reduction of 2% from repair only values. The difference in fat area fraction between the repair only and combined repair plus gel treatment group did not reach statistical significance ($P = .18$) (Fig. 6, *e*). The uninjured contralateral SSP fat content was minimal and similar within the repair only (0.6 + 0.2%) and the combined repair plus ECM gel (0.7 + 0.6%) groups. No statistical difference was detected between these groups. We did not detect any abnormal fibrosis in any of the tissue examined. Specifically, the collagen I area fraction was not affected by either repair only or combined repair plus gel treatment, when compared with normal muscle sections (Fig. 6, *f*). We did detect a significant difference in fiber cross-sectional area between treatment groups. Repair only treatment resulted in a 30 + 9.8% decrease in muscle fiber size when compared with uninjured contralateral controls, whereas combined tendon repair plus ECM gel injection resulted in a more modest decrease of 10 + 4.3% ($P = .005$) (Fig. 6, *g*).

The mRNA abundance (fold change) of genes associated with muscle degeneration (PPAR-γ, MURF1) was sensitive to repair only treatment (Fig. 7, *a*). PPAR-γ was significantly upregulated (3.15 + 2.44-fold change) ($P = .040$), whereas MURF1 was strongly downregulated (0.07 + 0.02-fold change) ($P = .042$) when compared with contralateral uninjured tissue. These genes were not significantly different from uninjured controls when examined in the combined repair plus gel injection group. The myogenic genes examined (Pax7, MyoG) were generally downregulated for both treatment groups (Fig. 7, *b*). Pax7 was significantly downregulated in both the repair only (0.08 + 0.07-fold change) and combined repair plus ECM gel group (0.05 + 0.04-fold change). However, although MyoD appeared downregulated when compared with uninjured controls tissue for both treatment groups, it only reached statistical significance for the repair only group (0.35 + 0.05-fold change).

Analysis of RNA-Seq data in EdgeR revealed a total of 40 differentially expressed genes (all upregulated) between the repair only group relative to uninjured controls, and 1 differentially expressed (downregulated) gene (DNAse1) between the combined repair plus gel group relative to control (Supplementary Table S1). Notably, in the repair only group, IPA detected the activation of the canonical adipogenesis pathway ($P < .0001$) due to 4 differentially expressed genes (PPAR-γ, LEP, KLF5, FABP4) and the activation of the canonical osteoarthritis (OA) pathway (*P*

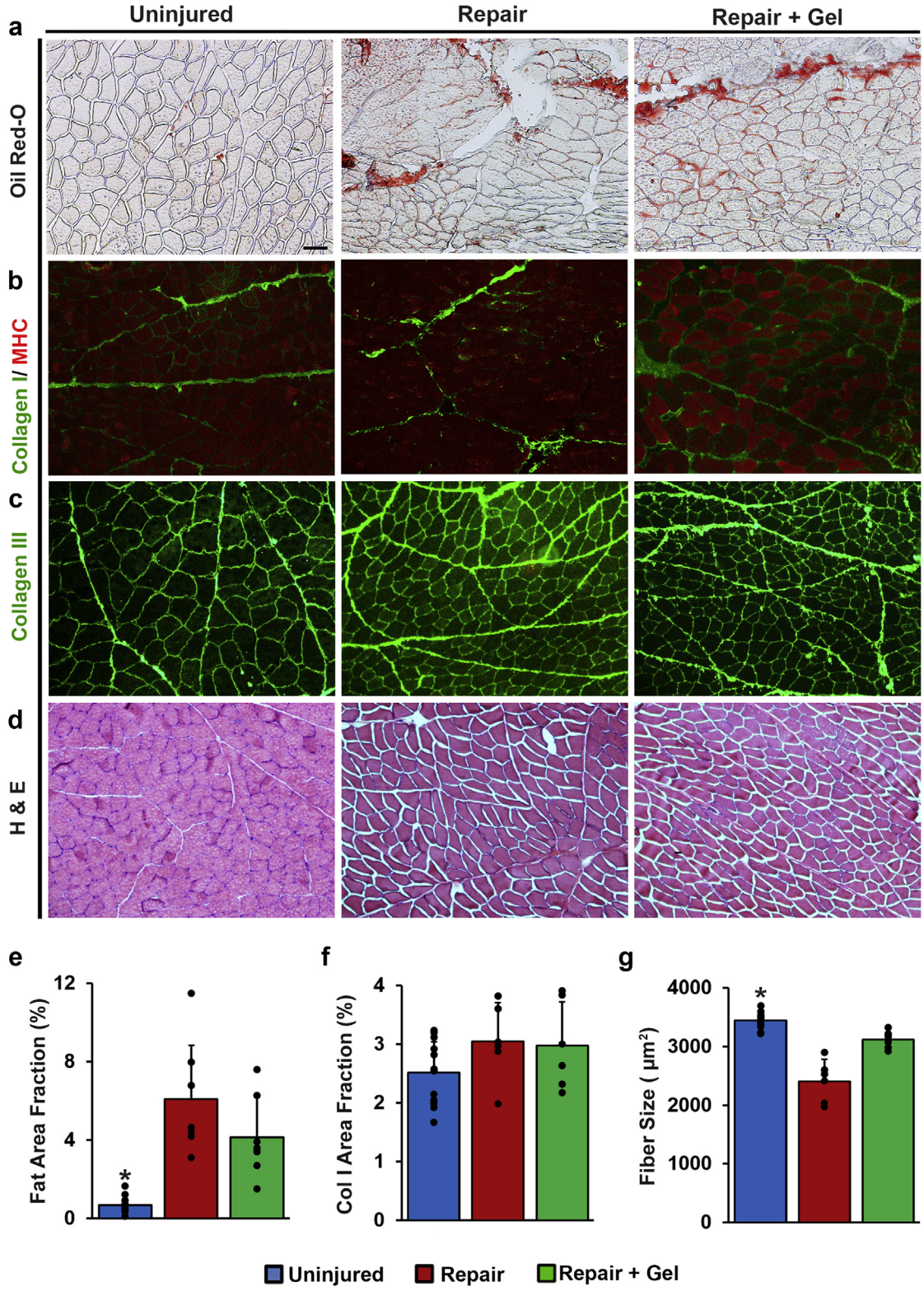

Figure 6 SSP muscle cross-sections were stained for (**a**) oil red-O, (**b**) collagen I (green) counterstained with MHC (red), (**c**) collagen III (green), and (**d**) hematoxylin and eosin (H&E). Representative 12 weeks after SSP repair images for the uninjured, repair only, and combined repair plus gel groups are presented. Scale bar = 100 μm unless noted. Repair only and combined repair plus ECM gel cross-sections were quantified to determine (**e**) area fraction collagen I, (**f**) area fraction oil red-O, and (**g**) muscle fiber cross-sectional area (μm^2). Group means + SD are presented; n = 6-7/group. *denotes statistically significant ($P < .05$) differences between groups. *SSP*, supraspinatus; *MHC*, myosin heavy chain; *ECM*, extracellular matrix; *SD*, standard deviation.

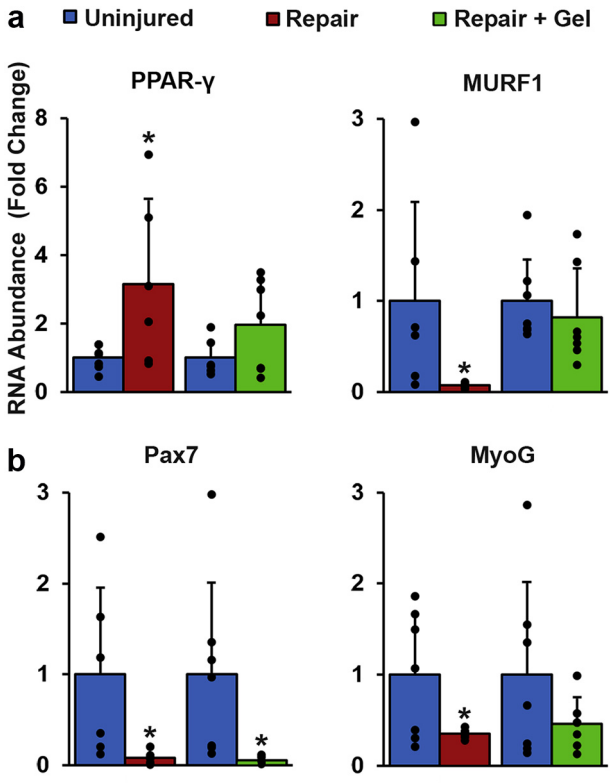

Figure 7 Comparison of relative gene expression for the repair only and combined repair plus ECM gel–injected groups using qRT-PCR. The expression of (**a**) adipogenesis (PPAR-γ), muscle synthesis (MURF1), (**b**) satellite cell dynamics (Pax7), and myogenesis (MyoG) were measured using muscle tissue harvested from the SSP of each animal tested. Expression is presented as fold change normalized to contralateral uninjured muscle expression. Group means + SD are presented, n = 6-7/group. *denotes statistically significant ($P < .05$) differences from uninjured controls. *ECM*, extracellular matrix; *qRT-PCR*, quantitative real time polymerase change reaction; *SSP*, supraspinatus; *SD*, standard deviation.

< .001) due to 4 differentially expressed genes (LEP, matrix metalloproteinase-12 [MMP-12], PPAR-γ, SSP1). IPA did not detect the activation of any pathways in muscle tissue collected from the combined repair plus ECM gel injection group.

Discussion

Our host-response findings using the rat model, which included functional, histologic, and gene expression measures, suggest that intramuscular ECM gel injection was well tolerated. We detected a significant increase in the expression of inflammatory cytokines (IL-6, IL-1) and macrophage markers (CD68) at 3 days after ECM injection. This finding is consistent with normal muscle wound healing, and although not a direct measure of macrophage presence, the increased expression of CD68 suggests macrophage infiltration in response to the presence of ECM fragments from the gel.[35,36] At 14 days postinjection, macrophage marker and inflammatory gene expression returned to basal levels suggesting that ECM injection did not elicit a foreign body response with chronic inflammation.[54] Future studies could benefit from a more extensive analysis of macrophage dynamics at the site of ECM gel injection. We did not observe foreign body giant cells within tissue sections at any of the time points. Consistent with normal wound healing, specifically remodeling and repair,[22] we observed a characteristic upregulation of key matrix (CoL I and III) and matrix-regulatory (TGF-β1) genes in response to intramuscular ECM matrix gel injection.[55] These genes remained upregulated into the second week but had returned to basal levels of expression at 56 days postinjection. Although matrix and matrix regulatory genes were upregulated in response to ECM injection, we did not observe any evidence of intramuscular fibrosis, suggesting normal matrix protein regulation during wound healing with balanced deposition of a new matrix and degradation of the damaged matrix.[6] Interestingly, we detected a significant increase in peak muscle force and mass in response to ECM gel injection. This outcome was unexpected, especially absent a finding of increased muscle fiber size, and warrants continued investigation.

The shoulder cuff repair findings indicate that the combination of tendon repair with ECM gel injection can have a positive effect on muscle atrophy. Although significant SSP atrophy occurred within both treatment groups when compared with contralateral uninjured SSP muscle, the use of combined tendon repair with ECM injection significantly reduced the amount of atrophy when compared with the tendon repair only group. Histologic evaluation revealed that the repair only group had significantly smaller myofiber cross-sectional area when compared with uninjured controls, which is consistent with the pathologic effect of muscle atrophy in other chronic rotator cuff injury models.[16,30] Alternatively, combining tendon repair with ECM gel injection resulted in the preservation of myofiber cross-sectional area in the SSP. Gene expression analysis using quantitative real time polymerase change reaction (RT-qPCR) provides a potential explanation for the differences in SSP atrophy and fiber size observed between the 2 treatments. We detected a reduction in MURF1, a well-known regulator of atrophy that acts as an important rate-limiting enzyme in protein degradation in skeletal muscle,[47] gene expression within the repair only group, whereas the expression was equivalent to normal uninjured muscle when examined in combined tendon repair with ECM gel injection tissue. The downregulation of MURF1 in the repair group, coupled with the absence of mass preservation of the SSP, suggests that tendon repair alone may be insufficient to sustain hemostasis of muscle protein synthesis in chronic RCT injury. The examination of genes related to myogenesis revealed that Pax7, a marker of satellite cell

activation, was significantly downregulated in both treatment groups. These results suggest that atrophic signaling may be inhibiting myogenic signaling in both treatment groups, which has been previously demonstrated in models of chronic RTC injury.[33]

Although it did not reach the level of statistical significance, fatty infiltration was modestly reduced (2%) in response to treatment with combined tendon repair with a single round of ECM gel injection. Cell signaling pathway analysis conducted using the transcriptome profiling results of both treated and uninjured SSP tissue detected the activation of key canonical signaling pathways in the repair only group, whereas none were found to be activated in uninjured SSP tissue or the ECM gel injection group. This suggests that ECM gel injection is possibly having a dampening effect on muscle tissue cellular signaling. In particular, within the adipogenic signaling pathway, 4 distinct transcription factors (PPAR-γ, LEP, KLF5, FABP4) were found to be significantly upregulated in response to tendon repair only treatment. These results are consistent with the observed increase in adipogenic gene expression in the repair only group with PCR. This story is further corroborated by a similar finding in the upregulation of FABP4 for the repair group, a protein that is involved in fatty acid uptake, transport, and muscle metabolism.[13,26] Interestingly, FABP4 has also been identified to be one of the key transcription factors affecting marbling in cattle meat, a condition with similarities to muscle fatty infiltration after rotator cuff injury.[25] An understanding of the transcriptional changes in FABP4 and abrogation of the adipogenesis pathway in response to ECM gel injection may explain the reduced level of fatty degeneration that we observed. In turn, it may provide a candidate target for combinatorial therapies that could be incorporated into ECM gels in order to enhance their efficacy.

Interestingly, we also detected upregulation of the OA pathway in the repair only group, but not in the ECM injection or uninjured SSP muscle groups. Specifically, MMP-12 was significantly upregulated in response to tendon repair only. MMPs, in general, and MMP-12, specifically, are associated with a number of degenerative diseases including rheumatoid arthritis.[7,38,40] In addition to degrading a wide range of substrates including those that compose the basal lamina, MMP-12 has also been shown to activate other matrix MMPs, further promoting matrix degradation and mechanical instability of the shoulder region.[4,38] This suggests that current repair techniques could potentially have the unintended consequence of creating tissue degradation and a mechanical environment that is associated with poor postoperative outcomes.[48] Abrogation of the OA pathway in the combined tendon repair with ECM injection group may warrant further investigation as it would appear to exert a protective effect on not just the injected muscle but the shoulder joint as well. We also detected significant downregulation of DNase1 within the ECM injection group. Although there have been no published findings concerning the role of DNase1 in rotator cuff injuries, the finding may be significant as DNase1 delivery has been shown to reduce extracellular traps that promote inflammatory and thrombosis cascades,[1] which could play a role in shoulder health.

A limitation to this study that deserves discussion was the lack of an early postinjection time point in the rabbit model. The 12-week endpoint examined in this study, although appropriate for the examination of recovery, did not allow us to make longitudinal comparisons between the repair only and repair plus ECM gel groups. As such, we cannot conclude whether the reduction in muscle atrophy that we observed in response to combined repair plus ECM gel treatment was the result of gel-induced muscle growth or simply a decrease in the rate of muscle atrophy when compared with repair only. Future studies will incorporate early postinjection time points in order to examine atrophy kinetics, as well as cellular (macrophages and other immune cells) and soluble factor (cytokines and growth factors) responses that may be responsible for the muscle atrophy differences we observed. Lastly, we did not use a sham injection as part of the repair only treatment group. As such we cannot separate the effect of the injection site injury from the presence of the ECM gel itself. However, the response to a sham PBS injection in the rat model was negligible, suggesting that the changes we observed in the rabbit model were predominately in response to the presence of the ECM gel.

To sum, it is well accepted that chronic rotator cuff tears are associated with a variety of pathologic changes to the skeletal muscle, including atrophy, fibrosis, and fatty infiltration.[8,18,32] Although means to repair chronically torn shoulder cuff tendons exist, unaddressed muscle pathologies can decrease the capacity for tendon healing, prevent full recovery of shoulder function, and are generally associated with poor outcomes.[8] We envision the use of the ECM gel material explored in this study as an adjunct to existing tendon repair strategies, in order to address both tendon and muscle injury in patients with chronically torn rotator cuffs. It is worth noting that the clinical use of ECM materials in muscle is not without precedent. Acellular ECM scaffolds have been used to improve the strength and range of motion in patients with volumetric muscle loss injuries.[12] Although we do not yet know the mechanism responsible for the improvement in muscle atrophy we observed, the ECM gel injection results when explored in a delayed SSP repair model were encouraging and warrant continued preclinical investigation in order to firmly establish safety and efficacy.

Conclusion

ECM gel injection elicited a host response that resulted in the elevation of wound repair gene expression at early time points, but did not lead to any pathologic changes in muscle architecture, suggesting tolerance by the host

environment. Furthermore, we detected a significant increase in muscle mass and contractile force in response to ECM gel injection, which warrants continued exploration. When examined in a delayed SSP repair model we observed a modest but measurable effect when ECM gel was used in combination with tendon repair. Specifically, intramuscular ECM gel injection mitigated SSP atrophy and abrogated the activation of key adipogenic and osteoarthritic signaling pathways. The results suggest that the short-term activation of wound healing pathways observed in the rat model is complemented by a longer-term positive effect on muscle atrophy and cellular signaling.

Acknowledgments

Research reported in this publication was supported by the National Institute of Arthritis And Musculoskeletal and Skin Diseases of the National Institutes of Health under Award Number 1R15AR073492-01 and the Arkansas Biosciences Institute.

Disclaimer

The other authors, their immediate families, and any research foundations with which they are affiliated have not received any financial payments or other benefits from any commercial entity related to the subject of this article.

Supplementary data

Supplementary data to this article can be found online at https://doi.org/10.1016/j.jse.2020.03.038.

References

1. Albadawi H, Oklu R, Raacke Malley RE, O'Keefe RM, Uong TP, Cormier NR, et al. Effect of DNase I treatment and neutrophil depletion on acute limb ischemia-reperfusion injury in mice. J Vasc Surg 2016;64:484-93. https://doi.org/10.1016/j.jvs.2015.01.031
2. Allen RE, Sheehan SM, Taylor RG, Kendall TL, Rice GM. Hepatocyte growth factor activates quiescent skeletal muscle satellite cells in vitro. J Cell Physiol 1995;165:307-12.
3. Aurora A, Garg K, Corona BT, Walters TJ. Physical rehabilitation improves muscle function following volumetric muscle loss injury. BMC Sports Sci Med Rehabil 2014;6:41. https://doi.org/10.1186/2052-1847-6-41
4. Chandler S, Cossins J, Lury J, Wells G. Macrophage metalloelastase degrades matrix and myelin proteins and processes a tumour necrosis factor-alpha fusion protein. Biochem Biophys Res Commun 1996;228:421-9.
5. Chia HN, Wu BM. Recent advances in 3D printing of biomaterials. J Biol Eng 2015;9:4. https://doi.org/10.1186/s13036-015-0001-4
6. Corcoran ML, Kleiner DE Jr, Stetler-Stevenson WG. Regulation of matrix metalloproteinases during extracellular matrix turnover. Adv Exp Med Biol 1995;385:151-9 [discussion: 79-84].
7. Curci JA, Liao S, Huffman MD, Shapiro SD, Thompson RW. Expression and localization of macrophage elastase (matrix metalloproteinase-12) in abdominal aortic aneurysms. J Clin Invest 1998;102:1900-10.
8. Deniz G, Kose O, Tugay A, Guler F, Turan A. Fatty degeneration and atrophy of the rotator cuff muscles after arthroscopic repair: does it improve, halt or deteriorate? Arch Orthop Trauma Surg 2014;134:985-90. https://doi.org/10.1007/s00402-014-2009-5
9. DeQuach JA, Lin JE, Cam C, Hu D, Salvatore MA, Sheikh F, et al. Injectable skeletal muscle matrix hydrogel promotes neovascularization and muscle cell infiltration in a hindlimb ischemia model. Eur Cell Mater 2012;23:400-12. discussion 12. https://doi.org/10.22203/ecm.v023a31
10. Di Schino M, Augereau B, Nich C. Does open repair of anterosuperior rotator cuff tear prevent muscular atrophy and fatty infiltration? Clin Orthop Relat Res 2012;470:2776-84. https://doi.org/10.1007/s11999-012-2443-z
11. Dobin A, Davis CA, Schlesinger F, Drenkow J, Zaleski C, Jha S, et al. STAR: ultrafast universal RNA-seq aligner. Bioinformatics 2013;29:15-21. https://doi.org/10.1093/bioinformatics/bts635
12. Dziki J, Badylak S, Yabroudi M, Sicari B, Ambrosio F, Stearns K, et al. An acellular biologic scaffold treatment for volumetric muscle loss: results of a 13-patient cohort study. NPJ Regen Med 2016;1:16008. https://doi.org/10.1038/npjregenmed.2016.8
13. Fischer H, Gustafsson T, Sundberg CJ, Norrbom J, Ekman M, Johansson O, et al. Fatty acid binding protein 4 in human skeletal muscle. Biochem Biophys Res Commun 2006;346:125-30. https://doi.org/10.1016/j.bbrc.2006.05.083
14. Gerber C, Fuchs B, Hodler J. The results of repair of massive tears of the rotator cuff. J Bone Joint Surg Am 2000;82:505-15.
15. Gerber C, Meyer DC, Schneeberger AG, Hoppeler H, von Rechenberg B. Effect of tendon release and delayed repair on the structure of the muscles of the rotator cuff: an experimental study in sheep. J Bone Joint Surg Am 2004;86:1973-82. https://doi.org/10.2106/00004623-200409000-00016
16. Gerber C, Meyer DC, Von Rechenberg B, Hoppeler H, Frigg R, Farshad M. Rotator cuff muscles lose responsiveness to anabolic steroids after tendon tear and musculotendinous retraction: an experimental study in sheep. Am J Sports Med 2012;40:2454-61. https://doi.org/10.1177/0363546512460646
17. Gerber C, Schneeberger AG, Hoppeler H, Meyer DC. Correlation of atrophy and fatty infiltration on strength and integrity of rotator cuff repairs: a study in thirteen patients. J Shoulder Elbow Surg 2007;16:691-6. https://doi.org/10.1016/j.jse.2007.02.122
18. Goutallier D, Postel JM, Bernageau J, Lavau L, Voisin MC. Fatty infiltration of disrupted rotator cuff muscles. Rev Rhum Engl Ed 1995;62:415-22.
19. Goutallier D, Postel JM, Lavau L, Bernageau J. [Impact of fatty degeneration of the suparspinatus and infraspinatus msucles on the prognosis of surgical repair of the rotator cuff]. Rev Chir Orthop Reparatrice Appar Mot 1999;85:668-76.
20. Grumet RC, Hadley S, Diltz MV, Lee TQ, Gupta R. Development of a new model for rotator cuff pathology: the rabbit subscapularis muscle. Acta Orthop 2009;80:97-103. https://doi.org/10.1080/17453670902807425
21. Gupta R, Lee TQ. Contributions of the different rabbit models to our understanding of rotator cuff pathology. J Shoulder Elbow Surg 2007;16:S149-57. https://doi.org/10.1016/j.jse.2007.05.002
22. Gurtner GC, Werner S, Barrandon Y, Longaker MT. Wound repair and regeneration. Nature 2008;453:314-21. https://doi.org/10.1038/nature07039

23. Harryman DT II, Mack LA, Wang KY, Jackins SE, Richardson ML, Matsen FA III. Repairs of the rotator cuff. Correlation of functional results with integrity of the cuff. J Bone Joint Surg Am 1991;73:982-9.
24. Hill M, Wernig A, Goldspink G. Muscle satellite (stem) cell activation during local tissue injury and repair. J Anat 2003;203:89-99. https://doi.org/10.1046/j.1469-7580.2003.00195.x
25. Hoashi S, Hinenoya T, Tanaka A, Ohsaki H, Sasazaki S, Taniguchi M, et al. Association between fatty acid compositions and genotypes of FABP4 and LXR-alpha in Japanese black cattle. BMC Genet 2008;9:84. https://doi.org/10.1186/1471-2156-9-84
26. Hotamisligil GS, Bernlohr DA. Metabolic functions of FABPs–mechanisms and therapeutic implications. Nat Rev Endocrinol 2015;11:592-605. https://doi.org/10.1038/nrendo.2015.122
27. Hurd SA, Bhatti NM, Walker AM, Kasukonis BM, Wolchok JC. Development of a biological scaffold engineered using the extracellular matrix secreted by skeletal muscle cells. Biomaterials 2015;49:9-17. https://doi.org/10.1016/j.biomaterials.2015.01.027
28. Jost B, Pfirrmann CW, Gerber C, Switzerland Z. Clinical outcome after structural failure of rotator cuff repairs. J Bone Joint Surg Am 2000;82:304-14.
29. Kasukonis B, Kim J, Brown L, Jones J, Ahmadi S, Washington T, et al. Codelivery of infusion decellularized skeletal muscle with minced muscle autografts improved recovery from volumetric muscle loss injury in a rat model. Tissue Eng Part A 2016;22:1151-63. https://doi.org/10.1089/ten.TEA.2016.0134
30. Killian ML, Cavinatto LM, Ward SR, Havlioglu N, Thomopoulos S, Galatz LM. Chronic degeneration leads to poor healing of repaired massive rotator cuff tears in rats. Am J Sports Med 2015;43:2401-10. https://doi.org/10.1177/0363546515596408
31. Klepps S, Bishop J, Lin J, Cahlon O, Strauss A, Hayes P, et al. Prospective evaluation of the effect of rotator cuff integrity on the outcome of open rotator cuff repairs. Am J Sports Med 2004;32:1716-22. https://doi.org/10.1177/0363546504265262
32. Kramer A, Green J, Pollard J Jr, Tugendreich S. Causal analysis approaches in Ingenuity Pathway Analysis. Bioinformatics 2014;30:523-30. https://doi.org/10.1093/bioinformatics/btt703
33. Lee YS, Kim JY, Kim HN, Lee DW, Chung SW. Gene expression patterns analysis in the supraspinatus muscle after a rotator cuff tear in a mouse model. Biomed Res Int 2018;2018:5859013. https://doi.org/10.1155/2018/5859013
34. Liao Y, Smyth GK, Shi W. featureCounts: an efficient general purpose program for assigning sequence reads to genomic features. Bioinformatics 2014;30:923-30. https://doi.org/10.1093/bioinformatics/btt656
35. Maquart FX, Pasco S, Ramont L, Hornebeck W, Monboisse JC. An introduction to matrikines: extracellular matrix-derived peptides which regulate cell activity. Implication in tumor invasion. Crit Rev Oncol Hematol 2004;49:199-202. https://doi.org/10.1016/j.critrevonc.2003.06.007
36. Maquart FX, Simeon A, Pasco S, Monboisse JC. [Regulation of cell activity by the extracellular matrix: the concept of matrikines]. J Soc Biol 1999;193:423-8.
37. Matsumoto F, Uhthoff HK, Trudel G, Loehr JF. Delayed tendon reattachment does not reverse atrophy and fat accumulation of the supraspinatus—an experimental study in rabbits. J Orthop Res 2002;20:357-63. https://doi.org/10.1016/S0736-0266(01)00093-6
38. Matsumoto S, Kobayashi T, Katoh M, Saito S, Ikeda Y, Kobori M, et al. Expression and localization of matrix metalloproteinase-12 in the aorta of cholesterol-fed rabbits: relationship to lesion development. Am J Pathol 1998;153:109-19.
39. Mauro A. Satellite cell of skeletal muscle fibers. J Biophys Biochem Cytol 1961;9:493-5.
40. Mengshol JA, Mix KS, Brinckerhoff CE. Matrix metalloproteinases as therapeutic targets in arthritic diseases: bull's-eye or missing the mark? Arthritis Rheum 2002;46:13-20. https://doi.org/10.1002/1529-0131(200201)46:1<13::aid-art497>3.0.co;2-s
41. Meyer DC, Rahm S, Farshad M, Lajtai G, Wieser K. Deltoid muscle shape analysis with magnetic resonance imaging in patients with chronic rotator cuff tears. BMC Musculoskelet Disord 2013;14:247. https://doi.org/10.1186/1471-2474-14-247
42. Oh JH, Chung SW, Kim SH, Chung JY, Kim JY. 2013 Neer Award: effect of the adipose-derived stem cell for the improvement of fatty degeneration and rotator cuff healing in rabbit model. J Shoulder Elbow Surg 2014;23:445-55. https://doi.org/10.1016/j.jse.2013.07.054
43. Rao N, Agmon G, Tierney MT, Ungerleider JL, Braden RL, Sacco A, et al. Engineering an injectable muscle-specific microenvironment for improved cell delivery using a nanofibrous extracellular matrix hydrogel. ACS Nana 2017;11:3851-9. https://doi.org/10.1021/acsnano.7b00093
44. Robinson MD, McCarthy DJ, Smyth GK. edgeR: a Bioconductor package for differential expression analysis of digital gene expression data. Bioinformatics 2010;26:139-40. https://doi.org/10.1093/bioinformatics/btp616
45. Rowshan K, Hadley S, Pham K, Caiozzo V, Lee TQ, Gupta R. Development of fatty atrophy after neurologic and rotator cuff injuries in an animal model of rotator cuff pathology. J Bone Joint Surg Am 2010;92:2270-8. https://doi.org/10.2106/JBJS.I.00812
46. Rubino LJ, Stills HF Jr, Sprott DC, Crosby LA. Fatty infiltration of the torn rotator cuff worsens over time in a rabbit model. Arthroscopy 2007;23:717-22. https://doi.org/10.1016/j.arthro.2007.01.023
47. Sandri M. Signaling in muscle atrophy and hypertrophy. Physiology (Bethesda) 2008;23:160-70. https://doi.org/10.1152/physiol.00041.2007
48. Sayed-Noor AS, Pollock R, Elhassan BT, Kadum B. Fatty infiltration and muscle atrophy of the rotator cuff in stemless total shoulder arthroplasty: a prospective cohort study. J Shoulder Elbow Surg 2018;27:976-82. https://doi.org/10.1016/j.jse.2017.12.021
49. Seif-Naraghi SB, Salvatore MA, Schup-Magoffin PJ, Hu DP, Christman KL. Design and characterization of an injectable pericardial matrix gel: a potentially autologous scaffold for cardiac tissue engineering. Tissue Eng Part A 2010;16:2017-27. https://doi.org/10.1089/ten.TEA.2009.0768
50. Seif-Naraghi SB, Singelyn JM, Salvatore MA, Osborn KG, Wang JJ, Sampat U, et al. Safety and efficacy of an injectable extracellular matrix hydrogel for treating myocardial infarction. Sci Transl Med 2013;5:173ra25. https://doi.org/10.1126/scitranslmed.3005503
51. Singelyn JM, Sundaramurthy P, Johnson TD, Schup-Magoffin PJ, Hu DP, Faulk DM, et al. Catheter-deliverable hydrogel derived from decellularized ventricular extracellular matrix increases endogenous cardiomyocytes and preserves cardiac function post-myocardial infarction. J Am Coll Cardiol 2012;59:751-63. https://doi.org/10.1016/j.jacc.2011.10.888
52. Tatsumi R, Anderson JE, Nevoret CJ, Halevy O, Allen RE. HGF/SF is present in normal adult skeletal muscle and is capable of activating satellite cells. Dev Biol 1998;194:114-28.
53. Terada N, Takayama S, Yamada H, Seki T. Muscle repair after a transsection injury with development of a gap: an experimental study in rats. Scand J Plast Reconstr Surg Hand Surg 2001;35:233-8.
54. Tidball JG. Mechanisms of muscle injury, repair, and regeneration. Compr Physiol 2011;1:2029-62. https://doi.org/10.1002/cphy.c100092
55. Tracy LE, Minasian RA, Caterson EJ. Extracellular matrix and dermal fibroblast function in the healing wound. Adv Wound Care (New Rochelle) 2016;5:119-36. https://doi.org/10.1089/wound.2014.0561
56. Ungerleider JL, Johnson TD, Rao N, Christman KL. Fabrication and characterization of injectable hydrogels derived from decellularized skeletal and cardiac muscle. Methods 2015;84:53-9. https://doi.org/10.1016/j.ymeth.2015.03.024
57. Zumstein MA, Jost B, Hempel J, Hodler J, Gerber C. The clinical and structural long-term results of open repair of massive tears of the rotator cuff. J Bone Joint Surg Am 2008;90:2423-31. https://doi.org/10.2106/JBJS.G.00677